Published online 16 October 2007 *Nucleic Acids Research, 2007, Vol. 35, No. 21* ***7109–7117***
doi:10.1093/nar/gkm773

In vivo assembling of bacterial ribosomal protein L11 into yeast ribosomes makes the particles sensitive to the prokaryotic specific antibiotic thiostrepton

Alberto García-Marcos, Antonio Morreale, Esther Guarinos, Elisa Briones, Miguel Remacha, Angel R. Ortiz and Juan P. G. Ballesta*

Centro de Biología Molecular Severo Ochoa, Universidad Autónoma de Madrid and Consejo Superior de investigaciones Científicas, Cantoblanco, Madrid 28049, Spain

Received August 13, 2007; Revised September 12, 2007; Accepted September 13, 2007

ABSTRACT

Eukaryotic ribosomal stalk protein L12 and its bacterial orthologue L11 play a central role on ribosomal conformational changes during translocation. Deletion of the two genes encoding L12 in *Saccharomyces cerevisiae* resulted in a very slow-growth phenotype. Gene *RPL12B*, but not the *RPL12A*, cloned in centromeric plasmids fully restored control protein level and the growth rate when expressed in a L12-deprived strain. The same strain has been transformed to express *Escherichia coli* protein EcL11 under the control of yeast *RPL12B* promoter. The bacterial protein has been found in similar amounts in washed ribosomes from the transformed yeast strain and from control *E. coli* cells, however, EcL11 was unable to restore the defective acidic protein stalk composition caused by the absence of ScL12 in the yeast ribosome. Protein EcL11 induced a 10% increase in L12-defective cell growth rate, although the *in vitro* polymerizing capacity of the EcL11-containing ribosomes is restored in a higher proportion, and, moreover, the particles became partially sensitive to the prokaryotic specific antibiotic thiostrepton. Molecular dynamic simulations using modelled complexes support the correct assembly of bacterial L11 into the yeast ribosome and confirm its direct implication of its CTD in the binding of thiostrepton to ribosomes.

INTRODUCTION

The ribosomal stalk is an essential and highly conserved ribosomal structure directly involved in translation supernatant factor functions (1). High-resolution cryo-EM models of bacterial (2) and eukaryotic (3) ribosomes show two clearly different stalk domains, a highly mobile elongated protrusion connected to a more static but conformational change prone base. The mobile domain of the prokaryotic stalk is formed by the CTD of either two or three dimers, depending on the species, of the acidic 12 kDa L7/L12 protein, which are linked to their corresponding NTDs by an unstructured and very flexible, hinge (4).

The L7/L12 NTDs interact with the protein L10 CTD and the complex binds to the conserved 23S rRNA GTPase associated region (GAR) formed by helices 42–44 through the L10 NTD. The GAR domain, together with the L10 NTD and the adjacently bound protein L11, forms the stalk base (4).

The L7/L12 CTDs, involved in the binding and function of the translation-soluble factors, are considered to be the functional domain of the stalk. The reason for the existence of multiple copies of the same active domain in the ribosome is not presently understood. Cross-linking results have led to the proposal that two of the L7/L12 CTDs are immobilized by interacting with protein L11 at the stalk base (5) suggesting that not all the copies have the same role. Moreover, it has recently been proposed that one L7/L12 CTD interacts with protein L11 and with the G' domain of elongation factor EFG, forming a previously observed arc-like connection at the stalk base (6).

The crystal structure of L11–GAR fragment complexes has confirmed a tight interaction of the protein CTD with the RNA (7,8), which is essential to determine its tertiary structure (9). In contrast, the L11NTD makes only limited contacts with the rRNA and shows a high mobility. It has been proposed that the L11NTD might function as a switch by reversibly binding to the rRNA and in this way determining the conformational changes detected in this important ribosomal domain during translocation (2,8,10–15). Each one of the two elongation factors, EFG and EFTu are supposed to recognize one specific conformation of the GAR domain, thus producing a

*To whom correspondence should be addressed. Tel: +34 91 4975076; Fax: +34 91 4974799; Email: jpgballesta@cbm.uam.es

different chemical modification protection pattern in this region (9). In spite of its structural and functional relevance, protein L11 is not absolutely essential for ribosome activity since bacterial strains lacking this protein are viable, although they grow very poorly (16).

In addition, protein L11 is also physiologically relevant due to its key role in the activity of thiostrepton and related compounds, a family of classical inhibitors of protein synthesis in prokaryotes (17,18). These compounds bind to the RNA, although their interaction is markedly increased by protein L11 (19,20). The primary target site of thiostrepton has been located in the 23S rRNA GAR domain (21,22), involving also the NTD of protein L11 (20,23). The drug and its analogues seem to bind to a cleft formed by the two stem-loops in the 3D structure of the GAR domain and by a proline-rich helix in the L11NTD (9,13,14,24,25). This model accounts for the resistance effects caused by A1067 methylation (26) and L11 mutations (27,28) as well as for A1095 chemical protection (21). These antibiotics seem to block the L11NTD–GAR complex in a fixed position, hindering conformational changes in the stalk base, which seem to be essential for elongation factor activity, inhibiting in this way protein synthesis (12–14,24). The eukaryotic ribosome is insensitive to thiostrepton and its resistance has been mainly linked to the presence of a G instead of an A at the position corresponding to 1067 in *E. coli* 23S RNA (29).

A model of the eukaryotic ribosomal stalk structure equivalent to that reported for prokaryotes is not yet available. Cryo-EM data show that the overall stalk structure is conserved in *S. cerevisiae* ribosomes (3,30). However, the characterization of its components indicates that the eukaryotic stalk is considerably more complex than the bacterial one (1,31). Thus, the acidic proteins have evolved into two families of independently coded proteins, P1 and P2, formed by a variable number of members depending on the eukaryotic organism; in *S. cerevisiae* there are two proteins of each type, P1α/P1β and P2α/P2β. In contrast to L7/L12, proteins P1 and P2 are not found in the ribosome as homodimers but mainly as P1/P2 heterodimers (32,33). In addition, protein P0 is notably larger than its bacterial L10 counterpart due to a C-terminal extension, which has structural and functional similarity to the acidic P1 and P2 proteins (34). Its higher structural complexity has apparently endowed the eukaryotic stalk with ribosome modulating capabilities than have not been detected in the bacterial one (31,35).

Eukaryotic protein L12 is the counterpart of prokaryotic L11, although their amino acid sequences show very low homology. In *S. cerevisiae*, protein ScL12 is encoded by two genes, *rpL12A* and *rpL12B*, which express an identical protein. Both genes can be simultaneously disrupted seriously affecting the cell growth but leaving the disrupted cells viable (36). The eukaryotic stalk base also undergoes important conformational changes during translation (37), suggesting that protein L12 must also have a relevant function.

In contrast to the proteins, the stalk rRNA moiety, the GAR domain, is functionally well conserved among all species. Thus, the bacterial and yeast GAR regions have been shown to be functionally interchangeable (38,39).

It has also been shown that bacterial protein L11 can bind *in vitro* to eukaryotic GAR rRNA fragment (29,40). In order to test whether this binding is functional in the cell, *E. coli* protein L11 has been expressed in a *S. cerevisiae* strain lacking protein L12. The results show that the bacterial protein is assembled into the yeast ribosome; however, its capacity to functionally complement the protein L12 absence is low, indicating that contrary to the RNA–protein interactions, the protein–protein interactions are poorly conserved. Nevertheless, in spite of its low functional activity, protein EcL11 makes the yeast ribosome partially sensitive to thiostrepton.

MATERIALS AND METHODS

Strains and growth conditions

Saccharomyces cerevisiae 6EA1 (*leu2-3,112, trp1-1, ura3-1, can1-100, RPL12A::KanMX4, RPL12B::HIS3*) originally called A6K1O-6EA1, was derived from strain W303 as previously described (36). Yeast were grown either in YEP (2% bacto-peptone, 1% yeast extract) or on minimal SD medium supplemented with appropriate nutritional requirements. In either media, either 2% glucose (YEPD, YNBD) or 2% galactose (YEPG, YNBG) were used as a carbon source.

Escherichia coli DH5α was grown in LB medium (2% bacto-tryptone, 1% NaCl, 1% yeast extract). For solid media, 2% agar was added in all cases.

Plasmids

Plasmids pFL38/L12A and pFL38-L12B, encoding yeast *RPL12A* and *RPL12B* genes, pYES2/L12, encoding the ScL12 ORF under the GAL1 promoter, and pFL38/L11A and pFL38/L11B, encoding EcL11 ORF under the control of the *RPL12A* and *RPL12B* flanking regions, were obtained as described in the Supplementary Data.

Enzymes and reagents

Restriction endonucleases and DNA modifying enzymes were purchased from Roche Molecular Biochemicals, MBI Fermentas, New England Biolabs and Amersham Pharmacia Biotech and were used as recommended by the suppliers. Oligonucleotides were synthesized by Isogen Bioscience. Recombinant DNA manipulation was carried out according to standard techniques.

Ribosome preparation and analysis

Ribosomes were obtained from cells broken with glass beads in the presence of a mixture of protease inhibitors (1 mM phenylmethylsulphonyl fluoride, 2.5 μg/ml leupeptin, pepstatin, antipain, aprotinin and chymostatin) as previously described and washed through a 20–40% sucrose gradient in 20 mM Tris–HCl, pH 7,4, 100 mM $MgCl_2$, 500 NH_4 Acetate, 5 mM β-mercapthoethanol (41).

Ribosomes from *E. coli* MRE600 were obtained as previously described (42). Polysomes were resolved in

10–40% sucrose gradients in 10 mM Tris–HCl, pH 7,4, 5 mM $MgCl_2$, 100 mM KCl, 5 mM β-mercapthoethanol, in a AH-627 Sorvall rotor at 23 000 r.p.m.

Inhibition of *in vitro* polyphenylalanine sysnthesis

The conditions for the inhibition of the *in vitro* of a poly(U)-dependent polyphenylalanine synthesis were described earlier (43).

Electrophoretic methods

Proteins were analysed by either 15% SDS–PAGE or isoelectrofocusing (IEF) following the procedure previously described (41). Yeast ribosomal stalk proteins were detected either by silver staining or using specific monoclonal antibodies (43). A rabbit serum raised against purified protein was used for bacterial L11.

Model building

The structure of *E. coli* L11 (EcL11) was taken from the Protein Data Bank (PDB ID 2AWB) (44). In the case of *S. cerevisiae* L12 (ScL12), the PDB file was 1K5Y (3). In this file, the structure of ScL12 presents only C alpha atoms; the remaining main and side chains were taken from the file 1S1I (37). The structure of RNA GAR domain was also taken from the 1S1I file, from *Haloarcula marismortui*, and was mutated into the one corresponding to *S. cerevisiae*. Finally, the structure of thiostrepton was extracted from the file 1OLN (25). With all these elements, the two ternary complexes were assembled as follows: using 1S1I as a template EcL11, ScL12 and RNA GAR domain were superimposed on their counterparts and the coordinates of thiostrepton were then exported. For comparative reasons, EcL11–EcGAR complex 2AW4 from *E. coli* was also considered (44).

Molecular dynamics simulations

All MD simulations were performed at a constant pressure and temperature (1 atm and 300 K) with an integration time step of 2 fs. SHAKE (45) was used to constrain all the bonds at their equilibrium distances. Periodic boundary conditions and the Particle Mesh Ewald (46) methods were used to treat long-range electrostatic effects. AMBER-99 (47) and TIP3P (47) force-fields were used in all cases. All the trajectories were performed using the AMBER 8 computer program and associated modules (48). The three models were built as discussed in the previous paragraph. The three complexes were hydrated by using boxes containing explicit water molecules, optimized, heated (20 ps) and equilibrated by following the trajectories by principal component analysis (PCA, see below). After equilibration, MD trajectories were continued for 25 ns of unrestrained MD simulation. Snapshots were sampled every 1 ps for the last 5 ns of the trajectories.

Thiostrepton-effective binding free energy to EcL11-EcGAR, ScL12-ScGAR and EcL11-ScGAR was qualitatively estimated using the MM-GBSA approach (45). The MM-GBSA method approaches free energy of binding as a sum of a Molecular Mechanics (MM) interaction term, a solvation contribution thorough a Generalized Born (GB) model, and a Surface Area (SA) contribution to account for the non-polar part of desolvation (49). These calculations were performed for each snapshot from the simulations using the appropriate module within AMBER 8.

At the same time, due to the considerable flexibility of the system observed during the simulation, the free energy landscape explored by thiostrepton and the inherent flexibility of each complex was studied by representing MM-GBSA interaction energies as a function of the first and second principal components obtained from PCA of the trajectories of the tertiary complex. The components were extracted from the spectral decomposition of covariance matrix using an averaged structure over the entire trajectory as reference. PCA computations were done using the C alpha atoms from the proteins and P atoms from the RNA together. For graphical representation, landscapes were generated using the Fields library (50) within R statistical package (51). This library uses a smoothing procedure based on the use of non-parametric regression to allow estimation of the expected energy landscape in those regions of the map not properly sampled during the simulation. The results should be interpreted more in a qualitative than in a quantitative sense.

RESULTS

Effect of *RPL12*A and *RPL12B* genes on cell growth

The yeast ribosomal protein ScL12 is not essential for cell viability, and *S. cerevisiae* 6EA1, a yeast strain totally lacking this ribosomal component, is able to grow in rich YEPD medium with a doubling time of around 5 h (36). The growth defect complementing capacity of the two genes encoding ScL12 in *S. cerevisiae*, *RPL2A* and *RPL12B*, was tested by transforming 6EA1 with pFL38 plasmids containing each one of them. Simultaneously, the effect of the *RPL12A* coding region under the control of the GAL1 promoter in plasmid pYES2 was also tested. The transformed strains were grown on liquid medium containing either galactose or glucose as a carbon source (Table 1). Transformation with *RPL12A* did not appreciably alter the 6EA1 growth rate, while the presence

Table 1. Effect of plasmid-encoded proteins on *S. cerevisiae* 6EA1 growth in liquid medium[a]

Strain	Transforming plasmid	YEPD medium	YEPG medium
W303	none	1.00	1.00
6EA1	none	3.20	3.64
6EA1	pFL38/L12A	3.11	3.50
6EA1	pFL38/L12B	1.20	1.27
6EA1	pYES2/L12	3.0	1.55
6EA1	pFL38/L11A	3.10	nt
6EA1	pFL38/L11B	2.90	nt

[a]The growth rate of the strains has been normalized considering as unit the doubling time of the parental W303 strain (94 min in YEPD and 110 min in YEPG). The values are the average of at least three measurements and have an average error of 5%.

of *RPL12B* allows the cells to grow at a rate close to that of the parental strain W303. Moreover, expression of the protein under the control of the GAL1 promoter in plasmid pYES2/L12 notably restored the 6EA1/GL12 strain cell growth when grown in galactose medium.

Differential expression of *RPL12A* and *RPL12B* genes

Ribosomes extracted from strains transformed with the different plasmids grown in YEPG medium were resolved by SDS–PAGE, and the presence of protein ScL12 was estimated by using a monoclonal-specific antibody (Figure 1A). The amount of protein detected in the respective samples is in agreement with the growth tests; thus, amounts of ScL12 similar to those in the parental W303 were present in 6EA1/L12B and 6EA1/GL12, while only traces were found in the cells expressing *RPL12A*. As expected, ScL12 is totally absent from the untransformed 6EA1. The presence of a cross-reacting band showing a higher molecular weight in 6EA1/GL12 cells might correspond to the product of either a premature in-phase initiation site or a partial suppression of the termination in the pYES2/L12 construct.

The ribosome-free supernatant fraction from the same transformed strains was also resolved by SDS–PAGE and western blotted using a monoclonal antibody specific for the conserved carboxyl end of the stalk P proteins. A clear increase of the band corresponding to the 12 kDa acidic protein P1/P2 as well as the presence of the 38 kDa P0 protein was detected only in the pFL38/L12A transformed strain and in the untransformed 6EA1 (Figure 1B). These results support the idea that the absence of protein ScL12 in these two strains apparently induces a destabilization of the stalk, which results in the accumulation of some of its components to the cytoplasm.

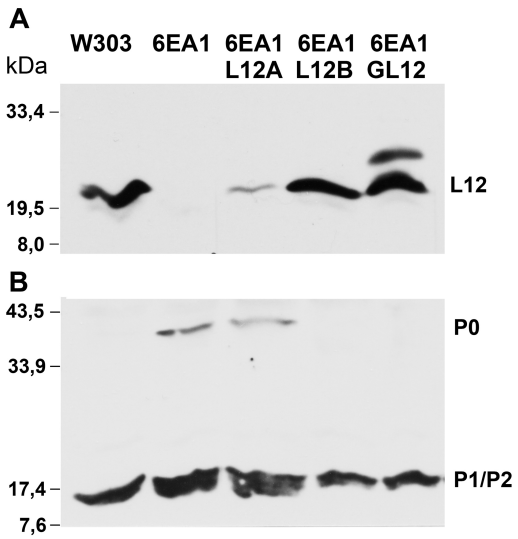

Figure 1. (**A**) Estimation of ScL12 in ribosomes using anti-ScL12 specific antibody. 40 µg of ribosomes extracted from cells expressing protein ScL12 from plasmids pFL38/L12A (6EA1/L12A) pFL38/L12B (6EA1/L12B) and pYES2/L12 (6EA1/GL12) were resolved by SDS–PAGE and the protein detected by immunobloting using an anti-ScL12 monoclonal antibody. (**B**) Western blot of S100 extracts from the same strains using a monoclonal antibody specific for the ribosomal stalk P proteins.

Effect of bacterial protein L11 on *S. cerevisisae* 6EA1 growth

To test whether the absence of yeast ScL12 can be complemented by its bacterial orthologue, the *E. coli* protein L11, plasmids pFL38/L11A and pFL38/L11B, containing the rpL11bacterial gene coding region under the control of the yeast *RPL12A* and *RPL12B* gene flanking regions, respectively, were used to transform *S. cerevisiae* 6AE1. Plasmids pFL38/L12B had a slight stimulatory effect of around 10% on the 6EA1 strain growth in liquid medium (Table 1).

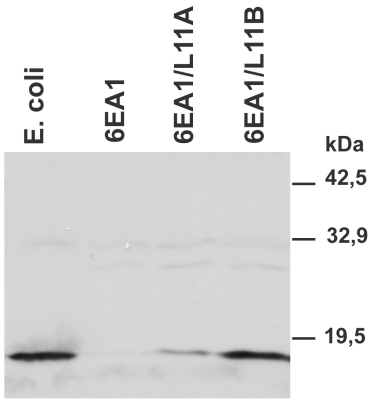

Figure 2. Protein EcL11 in ribosomes from *S. cerevisisae* 6EA1. Washed ribosomes from cells transformed with the constructs that contain the indicated proteins were resolved by PAGE–SDS and the protein detected using a specific antibody to protein EcL11. Equivalent amount of ribosomes were present in all samples, and particles from *E. coli* were used as a control.

Level of bacterial protein L11 expression in *S. cerevisiae* 6EA1

The amount of protein L11 present in the washed ribosomes from the transformed cells was estimated using a rabbit anti-L11 serum. The samples were resolved by PAGE–SDS and the protein detected by western blots (Figure 2). As in the case of protein ScL12 expression, bacterial L11 was only found in amounts equivalent to those present in the bacterial ribosomes when it is expressed from constructs carrying the *RPL12B* flanking regions. Since the ribosomes were washed following the standard procedures, these results indicate that L11 must have a similar affinity for the yeast and for the bacterial particle.

Effect of bacterial protein L11 on the yeast ribosomal activity

Sucrose gradients of cell extracts from *S. cerevisiae* W303, 6EA1, 6EA1-L12B and 6EA1-L11B showed that the absence of protein ScL12 results in the formation of halfmeres, which are suppressed by the expression of the native yeast protein but not by protein L11 (Figure 3). Moreover, a peak moving slower than the 40S subunits, which probably corresponds to accumulated pre-ribosomal

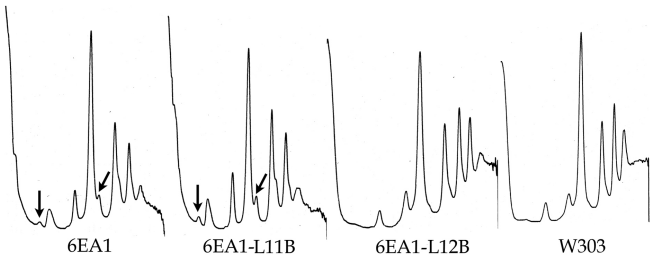

Figure 3. Sucrose gradient analysis of cell extracts. Extracts of *S. cerevisiae* 6EA1 expressing the indicated proteins were resolved by centrifugation through a 10–40% sucrose gradient. The corresponding A_{260} absorption profiles are shown. Arrows mark peaks corresponding to halfmers and possible pre-ribosomal particles.

Table 2. Polymerizing activity of ribosomes from different *S. cerevisiae* strains

Strain	W303	6EA1	6EA1-L11B	6EA1-L12B
Activity[a] (pmols of Phe polymerized)	21.4 ± 1.2	4.1 ± 0.6	7.1 ± 0.7	20.7 ± 2.2

[a]Average of three experiments.

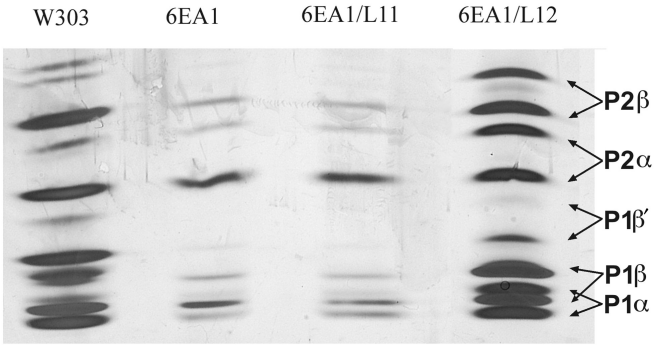

Figure 4. Isoelectrofocusing of ribosomes from the indicated strains. Ribosomes (100 µg) from W303 and 6EA1 expressing the indicated proteins were resolved by isoelectrofocusing (2.0 to 5.0 pH range) and the proteins detected by silver staining. The position of the different proteins is indicated.

particles, is present in similar extent in extracts from 6EA1 and 6EA1-L11B and not in 6EA1-L12B and parental W303 extracts (Figure 3). The *in vitro* translating capacity of washed ribosomes from different strains was directly tested in a poly(U)-dependent polyphenylalanine synthesis assay. As summarized Table 2, the ScL12-deficient ribosomes showed about 18% of the control activity. As expected, the presence of ScL12 almost fully restores the polymerizing activity of the particles while protein EcL11 causes an increase in the activity up to 32% of the control value.

Bacterial protein L11 does not restore the yeast ribosomal stalk composition

When the ScL12-depleted ribosomes from strain 6EA1 are resolved by isoelectrofocusing, a drastic reduction of the 12 kDa acidic proteins were found (Figure 4). The expression of the missing ScL12 protein from plasmid pFL38/L12B, restores the wild-type stalk composition

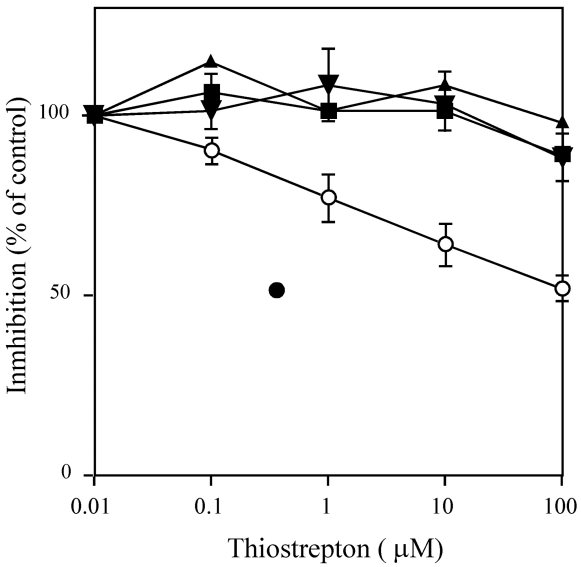

Figure 5. Inhibition of poly(U)-dependent polyphenylalanine synthesis by thiostrepton in extracts derived from *S. cerevisiae* W303 (filled square), 6EA1 (inverted filled triangle), 6EA1/L11 (open circle) and 6EA1/L12 (filled triangle). The IC_{50} for a *E. coli* extract is indicated (filled circle). The results are the average of three experiments. Since the error bars overlaps in many samples, we have included them only in data from strains 6EA1 and 6EA1/L11 in order to make the figure clearer. The standard deviation range was similar in the remaining samples.

while the expression of bacterial L11 has practically no effect on the amount of bound acidic proteins.

Bacterial protein L11 increases the sensitivity of yeast to thiostrepton

The antibiotic thiostrepton interferes with the bacterial elongation factor activity by binding to the GAR region in the 23SrRNA. As commented previously, protein L11 has been shown to have an important role in this process. In contrast, the eukaryotic translation machinery is insensitive to this inhibitor. In order to check whether protein L11 affects the response of the yeast ribosome to thiostrepton, an *in vitro* poly(U)-dependent protein synthesis assay derived from 6EA1 cells expressing either bacterial L11 or yeast L12 was used. As shown in Figure 5, the extract from cells expressing the bacterial protein are clearly inhibited ($IC_{50} \approx 100\,\mu M$) as compared with similar extracts from cells either containing or lacking ScL12, which were practically unaffected at the highest tested drug concentrations. Inhibition occurs, however, to a lesser extent than in bacterial systems, which have an IC_{50} around 0.2–0.5 µM.

Modelling the *E. coli* L11-*S. cerevisiae* rRNA complex

All the biochemical experimental data clearly show that the bacterial EcL11 binds very efficiently to the yeast rRNA, indicating a high conservation of the interaction site in both molecules. To gain a better understanding of the association of EcL11 with the yeast GAR domain at the molecular level, as well as the thiostrepton inhibitory activity, the structure of the

heterologous complex was modelled based on the reported crystal structure of the L11-GAR complex in *Thermotoga maritima* (8) and *E. coli* (44) using the nucleotide sequence of the yeast rRNA fragment (*S. cerevisiae* 26S rRNA fragment G1225-C1282). In order to find a structural justification of their different thiostrepton affinities, we compared our modelled EcL11–ScGAR complex with the equivalent complexes from the reported crystal structure of the *E. coli* (44) and from the *S. cerevisiae* 80S ribosome obtained by combining cryo-EM reconstruction with rRNA and protein molecular information (3). However, it became noticeable that protein ScL12 appears in the yeast 80S model in a position which is not consistent with the reported bacterial L11–GAR complex crystal structure (8). Therefore, the structure of the ScL12–ScGAR complex was remodelled. The binding of thiostrepton to the two modleled complexes, EcL11–ScGAR and ScL12–ScGAR, and the reported EcL11–EcGAR structure were analysed using molecular dynamic simulations (Figure 6).

Common analysis to test convergence on the dynamics trajectories was performed first, monitoring in particular, temperature, total energy and density. PCA analysis suggested a long equilibration period. Taking as reference the initial minimized structure, Root Mean Square Deviations (RMSD) were also calculated for the protein, RNA, thiostrepton and for the whole complex. The RMSD values for the individual components of the complex were similar for EcL11–EcGAR and EcL11–ScGAR, but higher for ScL12–ScGAR, suggesting a less structured complex.

The thiostrepton-binding energy landscapes as a function of the first two principal coordinates of the complexes are shown in Figure 6. The reference model (EcL11–EcGAR) presents a wide, low-energy region for antibiotic binding. Analysis of the conformational transitions in this space suggests a closure or hinge-like movement in the apical GAR hairpin loop near the thiostrepton-binding site and in the proline-rich helix of the protein in order to better accommodate the antibiotic. Smaller, low-energy areas are found for EcL11–ScGAR and ScL12–ScGAR complexes. The three representative structures selected present similar induced movements upon antibiotic binding, mostly involving improved ordering of the proline-rich helix lining the thiostrepton-binding site. From an energetic point of view, and considering that only relative numbers are relevant, the MM-GBSA analysis showed that the predicted thiostrepton-binding affinities for the EcL11–EcGAR, EcL11–ScGAR, ScL12–ScGAR correspond to −76.52, −67.88, −63.24 kcal/mol, respectively.

DISCUSSION

Individual disruption of the *RPL12A* and *RPL12B* genes has shown that their respective contribution to the cell ScL12 protein content is not identical (36). Thus, deletion of *RPL12B* results in a larger reduction of the growth rate and ScL12 content than deletion of *RPL12A*, however, the differences were not big (36). It was therefore unexpected to find a notable differences when the *S. cerevisiae* 6EA1, lacking both genes, was transformed with centromeric plasmids carrying each one of them. While *RPL12B* restores the growth rate of strain 6EA1 to almost the parental strain level, *RPL12A* has very little effect on the disruptant strain growth. Consistent with the effect on growth, the amount of protein detected in the pFL30/L12B transformed strain is much higher than in the strains transformed with pFL38/L12A. Similarly, a high amount of protein was detected when the *RPL12A* ORF was expressed from the GAL1 promoter in the pYES2 plasmid indicating that the differences between both genes are not due to the presence of unusual codons in the gene A copy.

Since sequencing confirmed the absence of mutations in the cloned genes, it is reasonable to assume that some additional regulatory elements not present in the plasmids, which we are trying to identify, are acting in the genomic gene copies, and are responsible for the different expression from the genomic and plasmid-borne gene copies.

The results in this report show that when protein EcL11, the bacterial orthologue of eukaryotic ribosomal protein ScL12, is expressed in yeast it can be transported to the nucleolus and assembled into the ribosome. Moreover, EcL11 seems to be able to bind to the yeast ribosome with roughly the same affinity as the homologous component, since it withstands the same washing protocol.

A high conservation of the large subunit rRNA GAR domain has been previously reported by showing that it is functionally interchangeable between prokaryotes and eukaryotes (38,39). Nevertheless, the low overall similarity of amino acid sequence of the corresponding proteins points to the conservation of the tertiary structure of the binding site. The crystal structure of the bacterial L11-GAR complex (7,8) clearly showed that the rRNA-binding site is located at the protein CTD, and a number of amino acids in and around the α5 helix, which are directly involved in the interaction, are conserved in prokaryotes and yeast (8). This part of bacterial L11CTD binds the minor groove of the GAR RNA 1067 stem primarily through protein backbone-RNA backbone interactions (8). Based on the bacterial crystal structure, a model for the EcL11–ScGAR complex has been generated (Figure 6B). Similarly, the ScL12–ScGAR model derived from the reported *S. cerevisiae* 80S ribosome has been modified to obtain a better fit with the bacterial structure (Figure 6C). Both modelled complexes as well the equivalent complex, EcL11–EcGAR (Figure 6A), obtained from the crystal structure of *E. coli* ribosome (44) have been used to analyse the binding of thiostrepton by molecular dynamic simulation. The resulting model for the interaction of the antibiotic with the control *E. coli* complex agrees with previous structural information (25) and specially the recently reported NMR analysis (14) and will be later discussed.

Regarding the protein–RNA interactions, the important hydrogen bonded pattern established between the base pair U1060(1234)-A1088(1262) and residues

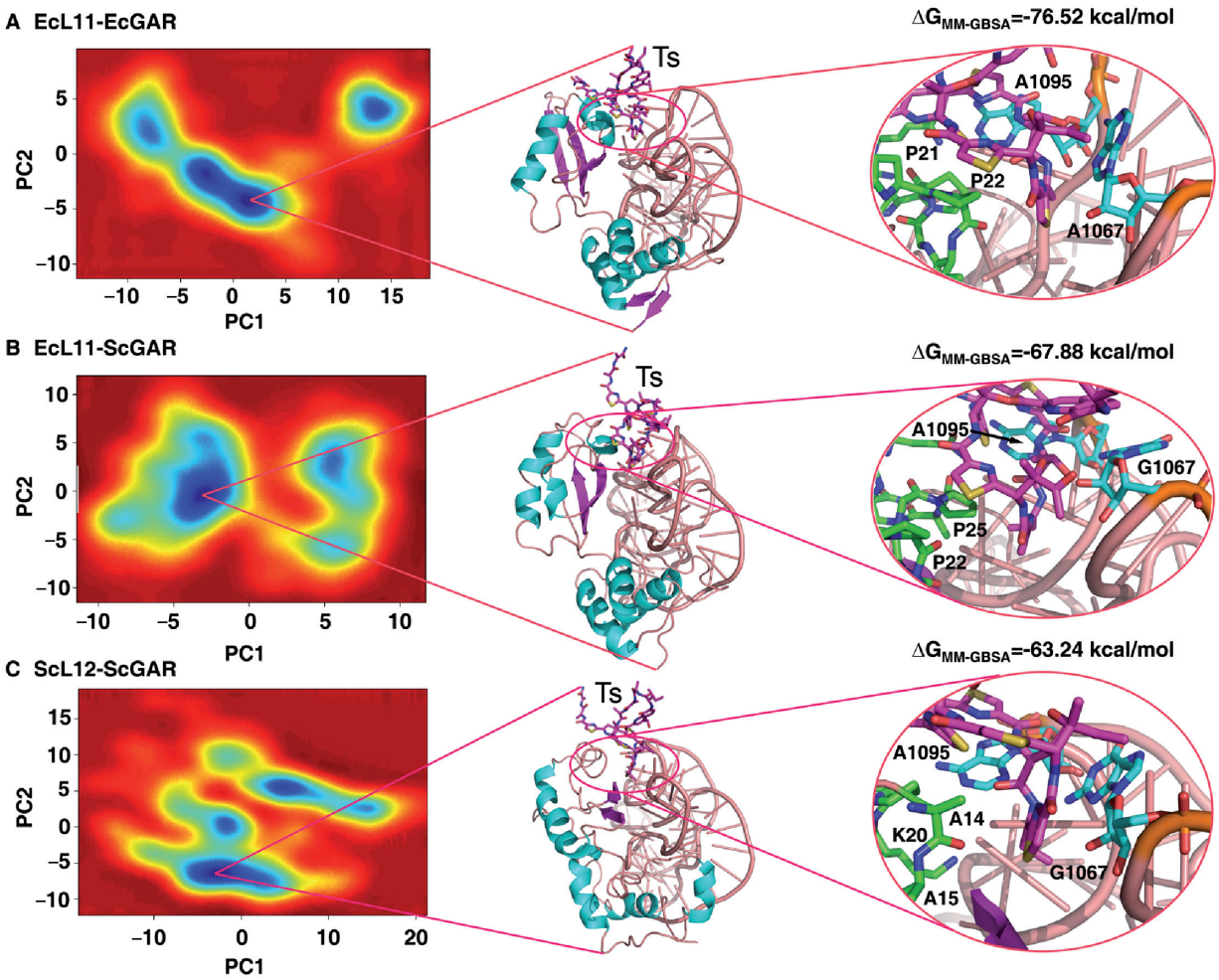

Figure 6. (**A**) Left panel: Thiostrepton free energy of binding to EcL11–EcGAR complex landscape as a function of two first principal components (C alpha and P atoms for the protein and RNA, respectively). Central panel: A representative structure corresponding to the minimum energy. The protein and RNA are coloured according to its secondary structure (α-helix, blue; β-sheet, magenta; RNA, lightpink). Thiostrepton (Ts) is coloured by atom type. Right panel: A close-up view of thiostrepton binding site. Main residues and bases affecting thiostrepton binding are highlighted as sticks and labelled with one-letter code and sequence number, with C atom coloured in green for the protein, cyan for RNA and magenta for thiostrepton. Hydrogen atoms have been omitted for clarity. (**B**) The same for EcL11–ScGAR complex. (**C**) The same for ScL12–ScGAR complex. In this case, equivalent residues between L11 and L12 proteins were obtained from structural alignment performed with the program MAMMOTH (52). In the three complexes, the energetic values correspond to the average obtained from the 5000 structures during the last 5 ns of each trajectory.

Gly130-Thr131 (8) are well-maintained throughout the simulation in EcL11–EcGAR and EcL11–ScGAR, and to a lesser extend in ScL12–ScGAR. In general, the protein–RNA interactions predicted in the model support the idea that the structural stability of the heterologous complex formed by the EcL11 CTD domain and the yeast GAR fragment cannot be very different from the homologous bacterial complex. The overall energy of the interactions is similar supporting that their stability must be comparable in agreement with the biochemical data from total ribosomes reported here and from *in vitro* studies using the GAR rRNA fragment (29).

In spite of its specific binding to the correct GAR RNA site, the bound EcL11 complements the ScL12 absence to a limited extent. The bacterial protein only causes an around 10% growth rate increase when it is expressed in the yeast strain lacking ScL12. Interestingly, although still low, the effect of EcL11 on the ribosome activity is proportionally higher, raising the activity of the ScL12-depleted ribosomes from 18 to 32% of the control. In contrast, the polysome profiles from the ScL12 depleted cells are practically unaltered by the presence of the bacterial protein and they show the accumulation of possible pre-ribosomal particles, which suggest that the exogenous protein might be less efficient at the level of ribosome assembly. All together, these results indicate that while the protein CTD–rRNA interactions responsible for the protein assembly are conserved, the evolution of the protein–protein interactions taking place mainly through the NTD during translation [with proteins L10 (4), L7/L12 (6) and elongation factors (2)] and ribosome assembly have negatively affected the EcL11 functionality in yeast.

Nevertheless, EcL11 has a significant effect on the sensitivity of the yeast ribosome to thiostrepton, a classical prokaryotic specific antibiotic inactive in eukaryotes. Yeast ribosomes, either carrying or lacking protein ScL12, are practically insensitive to this antibiotic while the hybrid ribosome carrying EcL11 showed an IC50 close to 100 μM. This value indicates that the hybrid ribosomes are still substantially more resistant than the bacterial systems, but clearly indicate that thiostrepton is able to interact with them and block protein synthesis.

The critical role of A1067 in *E. coli* 23S rRNA, or the equivalent position in other organisms, for the binding of thiostrepton to the ribosome has been convincingly demonstrated and the insensitivity of eukaryotes to this drug has been mainly related to the presence of a G in that position (29). However, when binding of the drug to naked rRNA was tested, the role of the nucleotide at position 1067 was found to be less relevant than expected, and the limited reduction caused by a G did not justify the high resistance of the eukaryotic ribosomes (39). It was concluded that in the ribosome the active conformation of the thiostrepton binding site is determined by the large rRNA GAR domain as well as by protein L11. In eukaryotes, protein L12 would either occlude or distort the site, hindering the drug binding.

Our results clearly indicate that binding of protein EcL11 is enough to substantially increase the sensitivity of the yeast ribosomes to the drug. The results of the molecular dynamic analysis of the thiostrepton interaction with the reported EcL11–EcGAR complex and with the modelled EcL11–ScGAR and ScL12–ScGAR complexes clearly indicated that the largest and smallest stabilization of thiostrepton correspond to EcL11–EcGAR (−76.52 kcal/mol) and ScL12–ScGAR (−63.24 kcal/mol), respectively, while the predicted binding affinities for EcL11–ScGAR (−67.88 kcal/mol) is someway in between. These results are in agreement with the available experimental data, which show that thiostrepton preferentially binds to the EcL11–EcGAR complex, but it is still able to bind to the EcL11–ScGAR complex at micromolar affinity. On the other hand, it does not apparently show significant affinity for the L12–RNA complex and, consequently, it is unable to inhibit the yeast ribosome. Visual inspection of thiostrepton bound to the three protein–RNA complexes indicates that while both the EcL11–EcGAR and EcL11– ScGAR complex share a similar set of interactions, the L12–RNA complex lacks a number of them (Figure 6). Significantly, in addition to the alteration at the important nucleotide at position 1067, the absence of the residues Pro21 and Pro22, mutated in both cases to Ala in L12, reduces the hydrophobic contact surface between the protein and the thiostrepton thiazolyl rings. This, together with the more open and polar site seen in L12 can help to explain the observed affinity differences.

ACKNOWLEDGEMENTS

This work was funded by Ministerio de Educación y Ciencia, Spain (BFU2006-00365 to J.P.G.B., GEN2003-206420-C09-08 and BIO2005-0576 to A.R.O.); Fundación Ramón Areces (institucional grant to CBMSO). We thank Dr Joachim Frank and Dr Christan Spahn for commenting on the reported models, Dr K. Nierhaus for a sample of *E. coli* protein L11 antiserum. Generous allocation of computer time at the Barcelona Supercomputer Center is gratefully acknowledged as well as M.C. Fernandez Moyano for technical assistance. Funding to pay the open access publication charges for this article was provided by Ministerio de Educación y Ciencia, Spain.

Conflict of interest statement. None declared.

REFERENCES

1. Gonzalo,P. and Reboud,J.P. (2003) The puzzling lateral flexible stalk of the ribosome. *Biol. Cell*, **95**, 179–193.
2. Agrawal,R.K., Linde,J., Sengupta,J., Nierhaus,K.H. and Frank,J. (2001) Localization of L11 protein on the ribosome and elucidation of its involvement in EF-G-dependent translocation. *J. Mol. Biol.*, **311**, 777–787.
3. Spahn,C.M., Beckmann,R., Eswar,N., Penczek,P.A., Sali,A., Blobel,G. and Frank,J. (2001) Structure of the 80S ribosome from *Saccharomyces cerevisiae*—tRNA- ribosome and subunit-subunit interactions. *Cell*, **107**, 373–386.
4. Diaconu,M., Kothe,U., Schlunzen,F., Fischer,N., Harms,J.M., Tonevitsky,A.G., Stark,H., Rodnina,M.V. and Wahl,M.C. (2005) Structural basis for the function of the ribosomal L7/12 stalk in factor binding and GTPase activation. *Cell*, **121**, 991–1004.
5. Traut,R.R., Dey,D., Bochkarlov,D.E., Oleinikov,A.V., Jokhadze,G.G., Hamman,B.D. and Jameson,D.M. (1995) Location and domain structure of *Escherichia coli* ribosomal protein L7/L12: site specific cysteine crosslinking and attachment of fluorescent probes. *Biochem.. Cell Biol.*, **73**, 949–958.
6. Datta,P.P., Sharma,M.R., Qi,L., Frank,J. and Agrawal,R.K. (2005) Interaction of the G' domain of elongation factor G and the C-terminal domain of ribosomal protein L7/L12 during translocation as revealed by cryo-EM. *Mol. Cell*, **20**, 723–731.
7. Conn,G.L., Draper,D.E., Lattman,E.E. and Gittis,A.G. (1999) Crystal structure of a conserved ribosomal protein-RNA complex. *Science*, **284**, 1171–1174.
8. Wimberly,B.T., Guymon,R., McCutcheon,J.P., White,S.W. and Ramakrishnan,V. (1999) A detailed view of a ribosomal active site: the structure of the L11- RNA complex. *Cell*, **97**, 491–502.
9. Bowen,W.S., Van Dyke,N., Murgola,E.J., Lodmell,J.S. and Hill,W.E. (2005) Interaction of thiostrepton and elongation factor-G with the ribosomal protein L11-binding domain. *J. Biol. Chem.*, **280**, 2934–2943.
10. Stark,H., Rodnina,M.V., Wieden,H.J., van Heel,M. and Wintermeyer,W. (2000) Large-scale movement of elongation factor G and extensive conformational change of the ribosome during translocation. *Cell*, **100**, 301–309.
11. Li,W., Sengupta,J., Rath,B.K. and Frank,J. (2006) Functional conformations of the L11-ribosomal RNA complex revealed by correlative analysis of cryo-EM and molecular dynamics simulations. *RNA*, **12**, 1240–1253.
12. Seo,H.S., Abedin,S., Kamp,D., Wilson,D.N., Nierhaus,K.H. and Cooperman,B.S. (2006) EF-G-dependent GTPase on the ribosome. Conformational change and fusidic acid inhibition. *Biochemistry*, **45**, 2504–2514.
13. Lee,D., Walsh,J.D., Yu,P., Markus,M.A., Choli-Papadopoulou,T., Schwieters,C.D., Krueger,S., Draper,D.E. and Wang,Y.X. (2007) The structure of free L11 and functional dynamics of L11 in free, L11-rRNA(58 nt) binary and L11-rRNA(58 nt)-thiostrepton ternary complexes. *J. Mol. Biol.*, **367**, 1007–1022.
14. Jonker,H.R., Ilin,S., Grimm,S.K., Wohnert,J. and Schwalbe,H. (2007) L11 domain rearrangement upon binding to RNA and thiostrepton studied by NMR spectroscopy. *Nucleic Acids Res.*, **35**, 441–454.

15. Kavran,J.M. and Steitz,T.A. (2007) Structure of the base of the L7/L12 stalk of the Haloarcula marismortui large ribosomal subunit: analysis of L11 movements. *J. Mol. Biol.*, **371**, 1047–1059.
16. Cundliffe,E., Dixon,P., Stark,M., Stöffler,G., Ehrlich,R., Stöffler-Meilicke,M. and Cannon,M. (1979) Ribosomes in thiostrepton-resistant mutant of *Bacillus megaterium* lacking a single subunit protein. *J. Mol. Biol.*, **132**, 235–252.
17. Vazquez,D. (1979) Inhibitors of protein synthesis. *Mol. Biol. Biochem. Biophys.*, **30**, 1–312.
18. Gale,E., Cundliffe,E., Reynolds,P.E., Richmond,M.H. and Waring,M.J. (1981) *The Molecular Basis of Antibiotic Action* John Wiley & Sons, London.
19. Thompson,J., Cundliffe,E. and Stark,M. (1979) Binding of thiostrepton to a complex of 23s rRNA with ribosomal protein L11. *Eur. J. Biochem.*, **98**, 261–265.
20. Bausch,S.L., Poliakova,E. and Draper,D.E. (2005) Interactions of the N-terminal domain of ribosomal protein L11 with thiostrepton and rRNA. *J. Biol. Chem.*, **280**, 29956–29963.
21. Egebjerg,J., Douthwaite,S. and Garrett,R.A. (1989) Antibiotic interactions at the GTPase associated centre within *E. coli* 23S RNA. *EMBO J.*, **8**, 607–611.
22. Thompson,J. and Cundliffe,E. (1991) The binding of thiostrepton to 23S ribosomal RNA. *Biochimie*, **73**, 1131–1135.
23. Xing,Y. and Draper,D.E. (1996) Cooperative interactions of RNA and thiostrepton antibiotic with two domains of ribosomal protein L11. *Biochemistry*, **35**, 1581–1588.
24. Porse,B.T. and Garrett,R.A. (1999) Ribosomal mechanics, antibiotics, and GTP hydrolysis. *Cell*, **97**, 423–426.
25. Lentzen,G., Klinck,R., Matassova,N., Aboul-ela,F. and Murchie,A.I. (2003) Structural basis for contrasting activities of ribosome binding thiazole antibiotics. *Chem. Biol.*, **10**, 769–778.
26. Thompson,J., Schmidt,F. and Cundliffe,E. (1982) Site of action of a ribosomal RNA methylase conferring resistance to thiostrepton. *J. Biol. Chem.*, **257**, 7915–7917.
27. Porse,B.T., Leviev,I., Mankin,A.S. and Garrett,R.A. (1998) The antibiotic thiostrepton inhibits a functional transition within protein L11 at the ribosomal GTPase centre. *J. Mol. Biol.*, **276**, 391–404.
28. Cameron,D.M., Thompson,J., Gregory,S.T., March,P.E. and Dahlberg,A.E. (2004) Thiostrepton-resistant mutants of Thermus thermophilus. *Nucleic Acids Res.*, **32**, 3220–3227.
29. Uchiumi,T., Wada,A. and Kominami,R. (1995) A base substitution within the GTPase-associated domain of mammalian 28 S ribosomal RNA causes high thiostrepton accessibility. *J. Biol. Chem.*, **270**, 29889–29893.
30. Gómez-Lorenzo,M.G., Spahn,C.M.T., Agrawal,R.K., Grassucci,R.A., Penczek,P., Chakraburtty,K., Ballesta,J.P.G., Lavandera,J.L., Garcia-Bustos,J.F. and Frank,J. (2000) Three-dimensional Cryo-EM Localization of EF2 in the *Saccharomyces cerevisiae* 80S Ribosome at 17.5 Å Resolution. *EMBO J.*, **19**, 2710–2718.
31. Ballesta,J.P.G. and Remacha,M. (1996) The large ribosomal subunit stalk as a regulatory element of the eukaryotic translational machinery. *Progr. Nucl. Acid. Res. Mol. Biol.*, **55**, 157–193.
32. Tchorzewski,M., Boguszewska,A., Dukowski,P. and Grankowski,N. (2000) Oligomerization properties of the acidic ribosomal P-proteins from Saccharomyces cerevisiae: effect of P1A protein phosphorylation on the formation of the P1A-P2B hetero-complex. *Biochim. Biophys. Acta*, **1499**, 63–73.
33. Guarinos,E., Remacha,M. and Ballesta,J.P.G. (2001) Asymetric interactions between the acidic P1 and P2 proteins in the *Saccharomyces cerevisiae* ribosomal stalk. *J. Biol. Chem.*, **276**, 32474–32479.
34. Santos,C. and Ballesta,J.P.G. (1995) The highly conserved protein P0 carboxyl end is essential for ribosome activity only in the absence of proteins P1 and P2. *J. Biol. Chem.*, **270**, 20608–20614.
35. Remacha,M., Jimenez-Diaz,A., Bermejo,B., Rodriguez-Gabriel,M.A., Guarinos,E. and Ballesta,J.P.G. (1995) Ribosomal acidic phosphoproteins P1 and P2 are not required for cell viability but regulate the pattern of protein expression in *Saccharomyces cerevisiae*. *Mol. Cell. Biol.*, **15**, 4754–4762.
36. Briones,E., Briones,C., Remacha,M. and Ballesta,J.P.G. (1998) The GTPase center protein L12 is required for correct ribosomal stalk assembly but not for Saccharomyces cerevisiae viability. *J. Biol. Chem.*, **273**, 31956–31961.
37. Spahn,C.M., Gomez-Lorenzo,M.G., Grassucci,R.A., Jorgensen,R., Andersen,G.R., Beckmann,R., Penczek,P.A., Ballesta,J.P. and Frank,J. (2004) Domain movements of elongation factor eEF2 and the eukaryotic 80S ribosome facilitate tRNA translocation. *EMBO J.*, **23**, 1008–1019.
38. Musters,W., Gonzalves,P.M., Boon,K., Raué,H.A., van Heerikhuizen,H. and Planta,R.J. (1991) The conserved GTPase center and variable V9 from *Saccharomyces cerevisiae* 26S rRNA can be replaced by their equivalent from other prokaryotes or eukaryotes without detectable loss of ribosomal function. *Proc. Natl Acad. Sci. USA*, **88**, 1469–1473.
39. Thompson,J., Muster,W., Cundliffe,E. and Dahlberg,A.E. (1993) Replacement of the L11 binding region within E. coli 23S ribosomal RNA with its homologue from yeast: *in vivo* and *in vitro* analysis of hybrid ribosomes altered in the GTPase centre. *EMBO J.*, **12**, 1499–1504.
40. El-Baradi,T.T.A.L., de Regt,V.C.H.F., Einerhand,S.W.C., Teixido,J., Planta,R.J., Ballesta,J.P.G. and Raué,H.A. (1987) Ribosomal proteins EL11 from *Escherichia coli* and L15 from *Saccharomyces cerevisiae* bind to the same site in both yeast 26S and mouse 28S rRNA. *J. Mol. Biol.*, **195**, 909–917.
41. Zambrano,R., Briones,E., Remacha,M. and Ballesta,J.P.G. (1997) Phosphorylation of the acidic ribosomal P proteins in *Saccharomyces cerevisiae*. A reappraisal. *Biochemistry*, **36**, 14439–14446.
42. Staehelin,T. and Maglott,D.R. (1971) Preparation of Escherichia coli ribosomal subunits active in polypeptide synthesis. *Methods Enzymol.*, **20**, 449–456.
43. Vilella,M.D., Remacha,M., Ortiz,B.L., Mendez,E. and Ballesta,J.P.G. (1991) Characterization of the yeast acidic ribosomal phosphoproteins using monoclonal antibodies. Proteins L44/L45 and L44′ have different functional roles. *Eur. J. Biochem.*, **196**, 407–414.
44. Schuwirth,B.S., Borovinskaya,M.A., Hau,C.W., Zhang,W., Vila-Sanjurjo,A., Holton,J.M. and Cate,J.H. (2005) Structures of the bacterial ribosome at 3.5 A resolution. *Science*, **310**, 827–834.
45. Ryckaert,J.P., Giccotti,G. and Berendsen,H.J.C. (1977) Numerical integration of the Cartesian equations of motion of a system with constraints: molecular dynamycs of n-alkanes. *J.Comput. Phys.*, **23**, 327–341.
46. Darden,T.A., York,D.M. and Pedersen,L.G. (1993) Particle mesh Ewald: an N_log(N) method for Ewald summs in large systems. *J. Chem. Phys.*, **98**, 10089–10092.
47. Cornell,W.D., Cieplak,P., Bayly,C.I., Gould,I.R., Merz,K.M., Ferguson,D.M., Spellmeyer,D.C., Fox,T., Caldwell,J.W. *et al.* (1995) A second generation force field for the simulation of proteins nucleic and organic molecules. *J. Am. Chem. Soc*, **117**, 5179–5197.
48. Case,D., Darden,T., Cheatham,T.E.,III, Simmerling,C., Wang,J., Duke,R., Luo,R., Merz,K., Wang,B. *et al.* (2004) *AMBER8* University of California, San Francisco.
49. Still,W.C., Tempczyk,A., Hawley,R.C. and Hendrickson,T. (1990) Semianalytical treatment of solvation for molecular mechanics and dynamics. *J. Am. Chem. Soc.*, **112**, 6127–6129.
50. Team,F.D. (2006) fields: Tools for spatial data. National Center for Atmospheric Research. Boulder, CO.
51. Team,R.D.C., (2006) R: A language and environment for statistical computing. R Foundation for Statistical Computing, Vienna, Austria. ISBN 3-900051-07-0.
52. Ortiz,A.R., Strauss,C.E. and Olmea,O. (2002) MAMMOTH (matching molecular models obtained from theory): an automated method for model comparison. *Protein Sci.*, **11**, 2606–2621.